Appl Petrochem Res (2016) 6:427–437
DOI 10.1007/s13203-016-0163-0

ORIGINAL ARTICLE

The advantage of ceria loading over V_2O_5/Al_2O_3 catalyst for vapor phase oxidative dehydrogenation of ethylbenzene to styrene using CO_2 as a soft oxidant

Venkata Ramesh Babu Gurram[1,2] · Siva Sankar Enumula[2] · Suresh Mutyala[2] · Ramudu Pochamoni[2] · P. S. Sai Prasad[2] · David Raju Burri[2] · Seetha Rama Rao Kamaraju[1,2]

Received: 24 February 2016 / Accepted: 9 June 2016 / Published online: 24 June 2016

Abstract The present work highlights the influence of ceria over vanadia/alumina for the oxidative dehydrogenation of ethylbenzene to styrene with CO_2 as a soft oxidant. Various weight loadings (0, 3, 5, and 7 %) of ceria were incorporated into 10wt % V_2O_5/Al_2O_3 catalyst by wet impregnation process. Structural and textural characterizations of the catalysts were performed by means of powder X-ray diffraction, temperature-programmed reduction, temperature-programmed desorption of CO_2, N_2 adsorption–desorption analysis. Over 10 % V_2O_5/Al_2O_3, ethylbenzene conversion decreases from 62 to 49 % in a spam of 12 h. Ceria-incorporated catalyst (3 % CeO_2/10 % V_2O_5/Al_2O_3) showed steady ethylbenzene conversion of nearly 65 % with a styrene selectivity of 96 % for a period of 12 h time. Improved catalytic activity observed on this catalyst can be attributed to the increase in the number of redox/active VO_x species after incorporation of ceria. The redox properties of 3 % CeO_2/10 % V_2O_5/Al_2O_3 and 10wt % V_2O_5/Al_2O_3 were examined by reaction of CO_2 in pulses on to the partially reduced catalysts. The spent catalysts were characterized using XRD & TPR analysis to assess the reason for the deactivation of catalysts.

Keywords Ceria · V_2O_5/Al_2O_3 · Oxidative dehydrogenation · Ethylbenzene · CO_2 as soft oxidant

Introduction

Styrene (ST) is an important monomer of many petrochemical industries for the production of polystyrene, styrene-acrylonitrile, styrene-butadiene rubber and acrylonitrile–butadiene–styrene [1]. ST is being produced via a commercial process using catalytic dehydrogenation of ethylbenzene (EB) with large quantity of steam as heat supplier, diluent and coke gasifier. The use of steam is highly energy consuming, and several alternatives to steam have been studied [2]. The high reaction temperature (873–973 K) and latent heat of steam condensation lead to excessive energy consumption for the steam-assisted EB dehydrogenation process. This process also shows the characters of the low atom economy, thermodynamic equilibrium limitations, short lifetime of catalysts, etc. [2, 3]. In this context, oxidative dehydrogenation with various types of oxidants like carbon dioxide, nitrous oxide, oxygen, sulfur dioxide and dry air gains momentum as alternatives for steam. Among these, carbon dioxide has enormous advantage because it reduces one of the major global warming gases via reverse water gas shift reaction (RWGSR). CO_2 employed in this reaction reacts with H_2 produced in the EB dehydrogenation reaction to yield CO and H_2O via RWGSR. Because of coupling of EB dehydrogenation reaction with RWGSR, enhancement in the catalytic activity is possible. Most importantly, in this process the CO_2 is converted to a useful co-product, carbon monoxide (2), which is one of the useful chemicals for Fischer–Tropsch synthesis and other organic transformations. Hydrogen can be recovered by the reaction of the

Electronic supplementary material The online version of this article (doi:10.1007/s13203-016-0163-0) contains supplementary material, which is available to authorized users.

✉ Seetha Rama Rao Kamaraju
ksramarao.iict@gov.in; ksramarao@iict.res.in

[1] CSIR-Academy of Scientific and Innovative Research (CSIR-AcSIR), New Delhi, India

[2] Catalysis Laboratory, Inorganic and Physical Chemistry Division, CSIR-Indian Institute of Chemical Technology, Hyderabad 500 007, India

formed CO with steam via water gas shift reaction (WGSR). Thus, CO_2 is considered as a promising soft oxidant to replace steam [4–7]. CO_2 has an advantage over steam in the form of equilibrium alleviation due to coupling of dehydrogenation reaction with RWGSR which increases the ST yield and also requires lower CO_2 consumption when compared to steam [8]. Reports say usage of oxygen overcomes thermodynamic limitations; the reaction can be operating at lower temperatures than the commercial process due to exothemicity of the process with oxygen. There are two main reactions occurred with O_2: (1) ODH reaction, (2) the coke gasification reaction [9–11]. The consumption of oxygen in EB dehydrogenation is very less (0.5 mol for a mole of EB). But the process with oxygen as an oxidant has not been realized yet because of significant loss of ST selectivity due to the production of carbon oxides and oxygenates [12].

EBD using CO_2 (3) follows via a two-step mechanism: the first one being a simple dehydrogenation of EB to ST (1) followed by RWGSR (2). Dehydrogenation of EB in the presence of CO_2 has attracted much attention after the pioneering works of Sato et al. [13] and Matsui et al. [14]. CO_2 can also be regarded as coke removal agent (4). Even though RWGSR is endothermic in nature, the energy required for oxidative dehydrogenation with CO_2 ($1.5–1.9 \times 10^5$ kcal) is lower by an order of one magnitude when compared to steam process (1.5×10^6 kcal) for the production of one ton of ST [15].

$$C_6H_5CH_2\text{-}CH_3 \longleftrightarrow C_6H_5CH{=}CH_2 + H_2 \qquad \Delta H_{298K} = 117.6\ kJmol^{-1} \quad (1)$$

$$CO_2 + H_2 \longleftrightarrow CO + H_2O \qquad \Delta H_{298K} = 41.6\ kJmol^{-1} \quad (2)$$

$$C_6H_5CH_2\text{-}CH_3 + CO_2 \longleftrightarrow C_6H_5CH{=}CH_2 + CO + H_2O \qquad \Delta H_{298K} = 159.2\ kJmol^{-1} \quad (3)$$

$$C + CO_2 \longleftrightarrow 2CO \quad (4)$$

EB dehydrogenation reaction without any oxidants (in the presence of inert gases) leads to nonselective products and facilitates faster deactivation of the catalyst. If CO_2 or N_2O is introduced, the deactivation of catalysts drops down drastically and selectivity towards ST not only increases but also sustains for prolonged times [16]. However, with increase in reaction temperature (above 873 K), the selectivity of ST considerably decreases due to thermal cracking of EB and other products. At higher temperatures, there is a possibility of the formation of higher amounts of toluene, benzene and other polyaromatics which deposit on the surface/pores of the sample that leads to severe fall in the ST selectivity [17, 18].

There are many reports on EB dehydrogenation; still a lot of research is needed to improve the process because of its huge industrial importance. Recently, Abhishek and et al. have reported improved CO_2 conversions in EB dehydrogenation over potassium- and sodium-doped Titania-Zirconia mixed oxide supports. The increase in the conversion of EB and CO_2 in case of doped TZ is because the dopants increase the stability of the catalysts by decreasing coke formation on the surface of the catalyst [19]. Sara and et al. have reported ethylene as the main coke precursor in EB dehydrogenation over $CrOx/Al_2O_3$ catalysts and the formation of coke is due to the formation of *para*-substituted aromatic species. They reported that precooking treatment is one of the options to inhibit undesired reactions (cracking, hydrogenolysis, and dealkylation) and thereby enhancement in the selectivity to ST [20]. Kovacevic et al. reported that ceria cubes exhibited a remarkable higher activity per m^2 for dehydrogenation of EB as compared to ceria rods and particles [21].

The physical and chemical properties of the support play a keen role in the ethylbenzene dehydrogenation reaction as reported by many researchers. Among several reported supports, alumina has major contribution because of their surface area, better redox properties, and high thermal stability. The molecular structure and reactivity of Vanadia supported alumina have been keenly investigated for few decades over dehydrogenation of EB [22–25]. Also, the CeO_2-based mixed oxides are effective catalysts for the oxidation of different hydrocarbons and for the removal of total organic carbon from polluted waters from different sources [26, 27]. The presence of CeO_2 promotes various catalytic reactions such as CO_2 activation [28], CO oxidation [29, 30], CO/NO removal [31] and low-temperature water–gas shift [32]. The success of ceria in various applications is mainly due to its unique properties like oxygen transport capacity, neutralizes the acidic sites of alumina, ability to shift easily between reduced and

oxidized states ($Ce^{3+} \leftrightarrow Ce^{4+}$) can create a better platform of acid–base bifunctionality with alumina which will play a pivotal role in EB dehydrogenation [33].

In our recent publications, utilization of CO_2 for EB dehydrogenation has been explained in detail over molybdenum- and cobalt-based catalysts. MoO_3 and Co_3O_4 supported on COK-12 (mesoporous silica) showed good activity towards EBD in the presence of CO_2 due to the formation of MoO_3 monolayer on the surface of the support [34] and the support COK-12 facilitates a better platform for Co_3O_4 [35]. Cobalt molybdenum bimetallic nitride catalyst supported on γ-Al_2O_3 showed high and stable activity in the presence of CO_2 and N_2. The high activity is due to the concurrent reactions of RWGSR and ammonia synthesis. The insitu generated ammonia (produced from N_2 and H_2) neutralizes the strong acidic sites of the catalyst which helps in maintaing the stable activity [36]. In continuation of our previous work, oxidative dehydrogenation of EB using CO_2 as a soft oxidant [34–36], the present study examines the promotive role of ceria to V_2O_5/Al_2O_3 catalyst.

Experimental

Materials

Ammonium metavanadate AR grade, NH_4VO_3 (M/s. LOBA Chemie, India), γ-Al_2O_3 (M/s. Harshaw, BET Surface area: 260 $m^2\ g^{-1}$), ammonium ceric nitrate AR grade, $H_8N_8CeO_{18}$ (M/s. SD fine chemicals, India), ethylbenzene (M/s. Sigma-Aldrich, anhydrous, 99.8 % purity) were used without further purification.

Catalyst preparation

10wt % V_2O_5/Al_2O_3 (VA) was prepared by dissolving requisite amount of ammonium metavanadate in Millipore water. After complete dissolution of the salt, finely powdered γ-Al_2O_3 was added. The excess water was evaporated on a hot plate under vigorous stirring. The resulting powder was dried overnight at 373 K and calcined at 773 K for 5 h with a ramping rate of 2 K min^{-1} in static air. 3, 5, and 7 weight % CeO_2 loaded V_2O_5/Al_2O_3 catalysts were prepared according to the procedure adopted for V_2O_5/Al_2O_3 catalysts. Briefly, requisite quantities of ammonium ceric nitrate and ammonium metavanadate were dissolved in Millipore water. After dissolution of salts, γ-Al_2O_3 powder was added to this solution and stirred the contents at 333 K for complete evaporation of water and dried at 373 K for overnight followed by calcination at 773 K for 5 h at a ramping rate of 2 K min^{-1} in static air. Final catalysts with corresponding loadings of ceria (0, 3, 5, and 7) were denoted as VA, 3VCA, 5VCA, and 7VCA, respectively.

Catalyst characterization

Powder X-ray diffraction patterns of the catalysts were recorded on a Ultima-IV X-ray diffractometer (M/s. Rigaku Corporation, Japan) using Ni filtered Cu Kα radiation (λ = 1.5406 Å) with a 2θ scan range of 10–80° and 2θ scan speed of 2° min^{-1} at 40 kV and 30 mA. Crystalline phases identified were compared with the reference data from International Center for Diffraction Data (ICDD) files. TPR analysis of catalysts was carried out using a quartz micro-reactor interfaced to a thermal conductivity detector (TCD) equipped gas chromatograph (M/s. CIC Instruments, India). Approximately, 50 mg of the catalyst sample is loaded in an isothermal zone of a quartz reactor (i.d. = 6 mm, length = 300 mm) and heated by an electric furnace to 573 K with ramping rate of 10 K min^{-1} and kept at that temperature for 1 h in helium gas flow (30 $cm^3\ min^{-1}$) to facilitate the desorption of physisorbed water. After degassing, the sample was cooled to 373 K and the helium gas was replaced with a reducing gas (5 % H_2 in argon) at a flow rate of 30 $cm^3\ min^{-1}$ and the temperature was linearly increased to 1073 K at a ramping rate of 10 K min^{-1} and maintained at the same temperature for 30 min. The hydrogen consumption was monitored by standard GC software. The basicity of the catalyst was measured by temperature-programmed desorption of CO_2 using an automated gas sorption analyzer, AUTOSORB-iQ (M/s. Quantachrome Instruments, USA). Prior to desorption, the catalyst has been pre-treated in He flow for 1 h at 573 K and cooled down to 373 K in the same helium flow. After that, the catalyst has been saturated with 10 % CO_2/He at 373 K for 0.5 h, followed by stripping with helium for 0.5 h to remove the physisorbed CO_2 at the same temperature. Then, the temperature was raised from 373 to 1073 K at a ramping rate of 10 K min^{-1} while maintaining the He flow (30 ml min^{-1}) and the desorbed gas was monitored with the TCD equipped GC. Re-oxidizability of the catalysts was examined by CO_2 pulse chemisorption experiment conducted at 873 K in a stainless steel reactor with 100 mg of the catalyst. Prior to this, the catalyst was reduced at 873 K in H_2 flow for 30 min. 100 µl volume of carbon dioxide was injected onto the catalyst sample in pulses through an assembled six-port valve and the outlet gas was analyzed by a TCD equipped GC-6890 (M/s. Agilent Corporation, USA) with Helium as a carrier gas and porapak T 80/100 column, 3 m length) [12]. The formation of coke was studied by CHNS analysis.

Catalyst activity studies

Catalytic activity study was performed in a fixed bed down flow quartz reactor at atmospheric pressure. 1 g of the catalyst was loaded at the center of the reactor with the help of two quartz wool plugs and subjected to pre-treatment with N_2 for 30 min at 873 K. Dehydrogenation of EB was performed in the temperature range of 723-923 K using CO_2 as a soft oxidant. The ratio of CO_2 to EB (ml/ml) was maintained as 30. EB was introduced by a liquid feed pump (M/s. B. Braun, Germany) at a feed rate of 8.2 mmol h^{-1} (1 ml/h). To assess the beneficial role of CO_2, a blank experiment with best catalyst under N_2 flow was also conducted. The products were collected at regular intervals in an ice cold trap and analyzed on a flame ionization detector (FID) equipped gas chromatograph, GC-17A (M/s. Shimadzu Instruments, Japan) using a capillary column, OV1-G43 (30 m length, 0.53 mm Inner diameter and 3 mm film thickness). The gaseous products were analyzed by injecting gas mixture into a thermal conductivity detector (TCD) equipped gas chromatograph, Agilent-6890 (M/S. Agilent Technologies, USA) having porapak-Q column (80–100 mesh size, 1 m length). EB conversion and ST selectivity are calculated as per the following Eqs. (5) and (6), respectively.

$$\mathrm{EB}_{\mathrm{Conversion}} = \left(1 - \frac{\text{ethylbenzene out}}{\text{ethylbenzene in}}\right) \times 100 \quad (5)$$

$$\mathrm{ST}_{\mathrm{Selectivity}} = \left(\frac{\text{Styrene out}}{\text{ethylbenzene in} - \text{ethylbenzene out}}\right) \times 100 \quad (6)$$

Results and discussion

Textual properties

The BET surface area and pore volume of the fresh catalysts are presented in Table 1. Surface area of the corresponding catalysts was measured by BET equation, which is inscribed below:

$$\frac{1}{\left[v_a\left(\frac{P_o}{p} - 1\right)\right]} = \left(\frac{C-1}{V_m C}\right)\frac{P}{P_o} + \frac{1}{V_m C}$$

where P is the partial vapor pressure of adsorbate gas in equilibrium with the surface at 77.4 K (b.p. of liquid nitrogen), in pascals; P_o is the saturated pressure of adsorbate gas, in pascals; V_a is the volume of gas adsorbed at standard temperature and pressure (STP) [273.15 K and atmospheric pressure (1.013×10^5 Pa)], in milliliters; V_m is the volume of gas adsorbed at STP to produce an apparent monolayer on the sample surface, in milliliters; and C is the dimensionless constant that is related to the enthalpy of adsorption of the adsorbate gas on the powder sample.

Incorporation of 10 weight % V_2O_5 decreases the BET surface area of alumina (260 m^2 g^{-1}) to 230 m^2 g^{-1} due to the blocking of support pores by V_2O_5 particles. After ceria addition, the surface areas further decreased to 183, 146, and 144 m^2 g^{-1} for 3VCA, 5VCA and 7VCA catalysts, respectively. For 7VCA, there was not much noticeable loss in surface area when compared to 5VCA, indicating that the alumina surface is saturated with vanadia and ceria particles in 5VCA and 7VCA. A similar trend in pore volume is also observed. It clearly says that the ceria particles after 5VCA were simply settling down on the surface of alumina. The normalized surface area values (surface area of catalyst/surface area of support component) of all the catalysts are close to unity, which is an identification of homogeneous distribution of VO_x species [37].

XRD analysis

XRD patterns of the catalysts VA, 3VCA, 5VCA, and 7VCA catalysts are shown in Fig. 1. XRD patterns of VA show that four diffraction peaks at 2θ values of 37.5 (311),

Table 1 Ceria loading, corresponding textual properties and ethylbenzene conversions of VA, 3VCA, 5VCA, and 7VCA catalysts

Catalyst	Ceria loading (wt %)	Surface area (m^2/g)[a]	Surface area (m^2/g-support)	NS^b_{BET}	Pore volume (cc/g)[c]	X (EB) (%)[d]
VA	0	230	256	0.90	0.29	65.3
3VCA	3	183	210	0.87	0.21	69.1
5VCA	5	146	172	0.85	0.19	68.4
7VCA	7	144	174	0.83	0.18	65.6

[a] BET Surface area

[b] Normalized BET surface area

[c] Total pore volume at relative pressure P/P_o by single point method

[d] *X* ethylbenzene conversion. *Reaction conditions* 1 g catalyst, $T = 600$ °C, 1 atm, 1 ml/h EB flow, 30 ml/min CO_2 flow

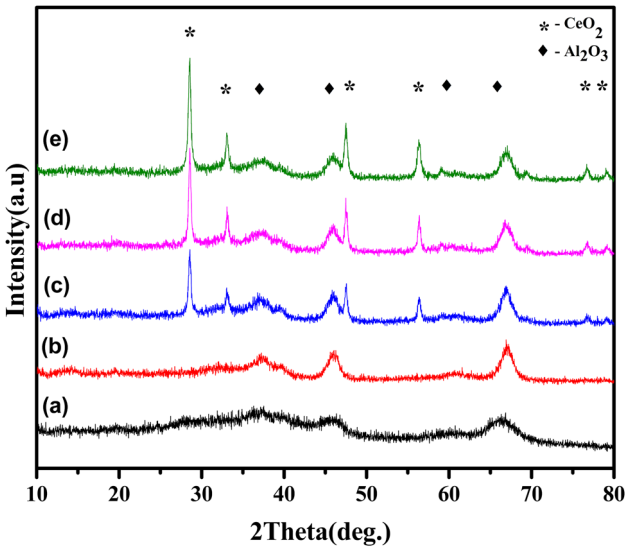

Fig. 1 Powder XRD patterns of *a* γ-Al_2O_3, *b* VA, *c* 3VCA, *d* 5VCA, and *e* 7VCA catalysts

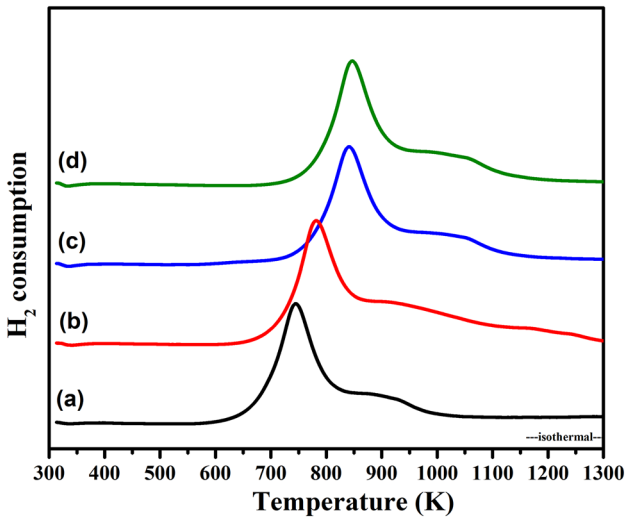

Fig. 2 TPR patterns for *a* VA, *b* 3VCA, *c* 5VCA, and *d* 7VCA catalysts

45.6 (400), 60.5 (511) and 66.6 (440) correspond to γ-Al_2O_3 (ICDD No 50-0741), and no diffraction peaks corresponding to crystalline vanadia were observed, suggesting that vanadia is highly dispersed or in amorphous phase on the surface of alumina. Assuming a cross-sectional area of V-atom as 6.803×10^{-20} m^2, γ-Al_2O_3 with a surface area of 260 m^2 g^{-1} can accommodate above 50 wt % of V2O5 in a monolayer provided that the pore size of alumina is sufficient enough to accommodate V-atoms. With incorporation of ceria on VA, diffraction peaks corresponding to ceria at 2θ values of 28.5 (111), 33.0 (200), 47.5 (220), 56.3 (311), 59.1 (222), 69.4 (400), 76.7 (331), and 79.1 (420) were observed at a ceria weight loading of 3 %. The diffraction planes are in good agreement with ICDD No. 81-0792. With increase in the composition of ceria from 3 to 7 %, the intensity of diffraction peaks of ceria increases due to the increase in crystallinity of the catalysts. Incorporation of large size of Ce^{3+} ions in the vacant positions of small size alumina might be the reason for the presence of both alumina and ceria peaks in XRD spectrum [38]. The CeO_2 crystallite size calculated from Debye–Scherrer equation in all the ceria promoted catalysts comes to be ~50 nm. From XRD results, it is clear that alumina surface is covered by VO_x species and further addition of CeO_2 was settling down on the surface.

H_2-TPR results

To investigate the reducibility of the vanadium species dispersed on the support in the presence of ceria, VCA samples are subjected to temperature-programmed reduction (TPR) in the temperature range of 373–1173 K and the results are compiled in Fig. 2. TPR patterns of supported vanadium species result in yielding a single T_{max} at around 723–873 K depending on the nature of support. VO_x species is more easily reduced when deposited on ZrO_2 (T_{max} = 817 K) rather than on MgO surface (T_{max} = 933 K) [39, 40]. The significantly higher temperature needed for the reduction of VO_x species on MgO is due to the higher degree of interactions between VO_x and oxidic support which are confirmed by the identification of MgV_2O_6 and VMgO phases [41].

Shiju and et al. reported that lower vanadia loadings (2–10 %) reveal a broad reduction peak below 773 K. A decrease in the reduction temperature with increase in the vanadia loading was observed by them. The shift in T_{max} value with increasing vanadia loading results from the reduction of monomeric, dimeric or low oligomeric surface vanadia species. The shift in reduction peaks with increase in vanadium content may be ascribed to the progressive increase in polymeric vanadium species [22]. In our present study, the catalyst VA showed a high intense signal at around 803 K and another small intense shoulder peak at around 943 K. The low-temperature peak might be attributed to the reduction of dispersed surface vanadium species mostly due to the presence of monomeric phase (tetragonal phase) of the vanadia species, while the high temperature peak should be ascribed to the reduction of bulk V_2O_5-like V^{5+} species with lower intensity [41–43]. With incorporation of 3 weight % of ceria (3VCA), T_{max} shifted to higher temperature suggesting increase in the interaction between CeO_2 and VO_x. With increase in ceria loading (5VCA), T_{max} increases to 906 K due to further increase in interactions between CeO_2 and VO_x species. 7VCA catalyst also showed same kind of reduction behavior

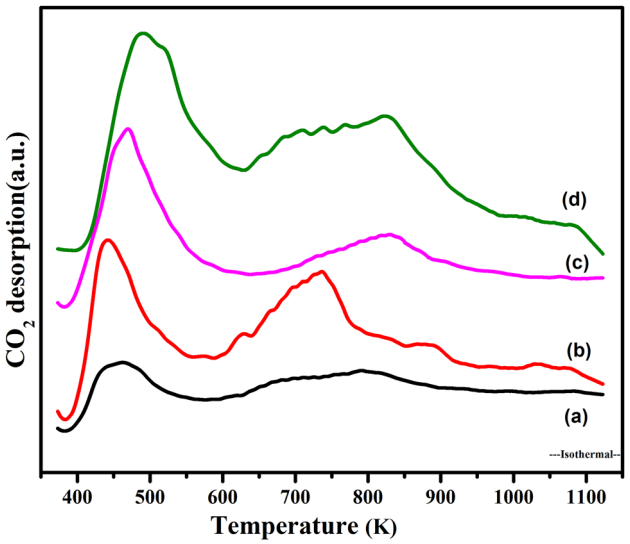

Fig. 3 CO_2 TPD profiles for *a* VA, *b* 3VCA, *c* 5VCA, and *d* 7VCA catalysts

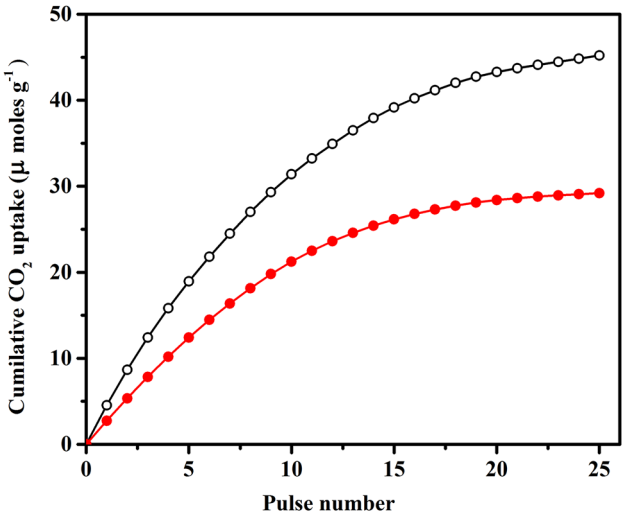

Fig. 4 CO_2 pulse treatment for partially reduced *a* (*dark circle*) VA, *b* (*open circle*) 3VCA catalysts

indicating the saturation of interaction between ceria and vanadia in 5VCA catalyst.

CO_2-TPD results

To explain surface basicity of samples, CO_2-TPD profiles are recorded (Fig. 3). CO_2-TPD profile of VA shows an intense peak at ~473 K and two shoulder peaks in the range of 673–873 K. The two peaks at ~443 and 673–873 K ascribed to the presence of weak and moderate basic sites. CO_2-TPD profile of 3VCA sample shows the presence of large population of week basic sites (T_{max} ~440 K) and also moderate basic sites (T_{max} ~735 K) compared to VA. It appears that incorporation of ceria increases basicity of VA. Similar kind of desorption behavior was observed from the CO_2-TPD profiles of 5VCA and 7VCA, which shows the presence of weak and moderate basic sites (T_{max} ~473 and 833 K), respectively. Shifting of T_{max} towards right hand side (higher T_{max}) might be attributed to increased interactions between CeO_2 and VO_x in 5VCA and 7VCA compared to 3VCA. The increase in the number of surface basic sites can be attributed to the doping effect as it is evinced from XRD results that surface was covered with ceria and the vanadia, dispersed on the alumina surface. The surface basicity is one of the major factors for the adsorption of CO_2 [19].

CO_2 pulse chemisorption study

CO_2 pulse injection experiments are planned to know the oxidizing power of a catalyst. Since EB dehydrogenation has been conducted with CO_2 as soft oxidant, it is a good idea to choose CO_2 as a probe molecule to assess the oxidizing power of a catalyst [12]. The selection of temperature for CO_2 pulse injection experiments is based on the EB dehydrogenation reaction temperature. Thus, CO_2 pulse chemisorption experiments were conducted at 873 K. Since the catalyst prior to the CO_2 chemisorption has been reduced in H_2 flow, during the pulse chemisorption, CO_2 gets reduced to CO and the lower oxidation of metal oxide (V/CeO_x) gets oxidized. The amount of CO produced is same as that of CO_2 consumed during the successive injections of CO_2 pulses at 873 K on a partially reduced catalyst with and without ceria. The amount of CO_2 consumed against pulse number is shown in Fig. 4. The reactivity of a catalyst towards CO_2 pulse reaction reflects its re-oxidizability of reduced surfaces. CO_2 uptake over 3VCA catalyst is conspicuously higher than that on VA implying that the oxidizing power of 3VCA catalyst is 55 % greater than that of VA. This clearly indicates that the amount of CO_2 conversion over 3VCA is larger compared to VA. The unique combination of excellent oxygen storage/release capacity features of CeO_2 and the oxidizing ability of dispersed vanadium oxide is an expected result which reflects in yielding good EB conversions with CO_2.

Reaction results

EB dehydrogenation reaction was carried out in vapor phase at atmospheric pressure over different weight loadings of ceria by maintaining the vanadium loading constant (VA, 3VCA, 5VCA, and 7VCA) at temperatures ranging from 723 to 923 K using CO_2 as a soft oxidant. The catalytic activity is shown in Figs. 5 and 6. Figure 5 depicts EB conversion whereas Fig. 6 depicts ST selectivity. Since

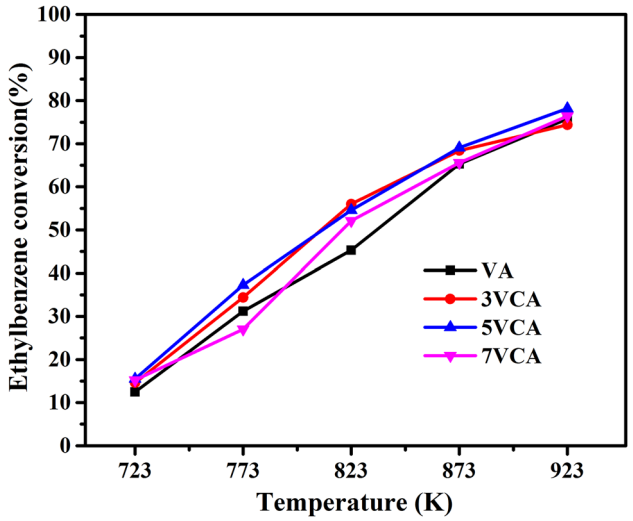

Fig. 5 Ethylbenzene converison over different ceria loadings VA, 3VCA, 5VCA, and 7VCA catalysts

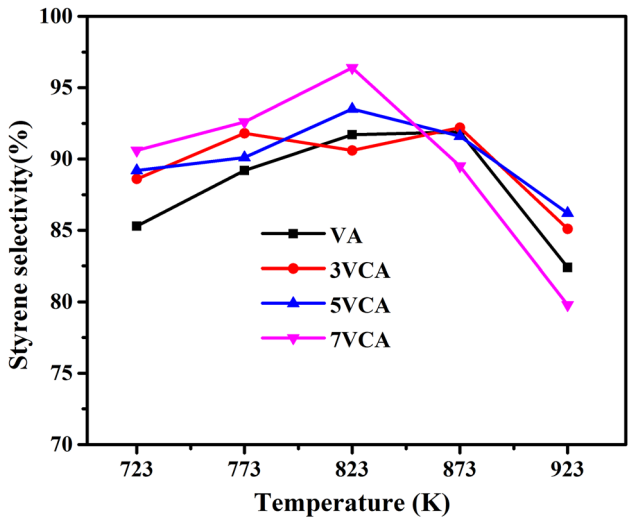

Fig. 6 Styrene selectivity over different ceria loadings VA, 3VCA, 5VCA, and 7VCA catalysts

EB dehydrogenation is an endothermic reaction, with increasing reaction temperature an increase in the EB conversion was observed. The catalyst VA exhibited low EB conversions at 723, 773, and 823 K. Further increase in temperatures (873 and 923 K) elevates the EB conversion to higher values, but the selectivity towards ST drops down due to the formation of more byproducts at higher temperatures. With the addition of 3 % ceria to VA (3VCA), a slight increase in EB conversion was observed that of VA. The slight improvement in EB conversion and ST selectivity is might be due to the enhancement of redox properties of the active species of VA catalyst with the addition of ceria. In this connection, it is worth to mention that the

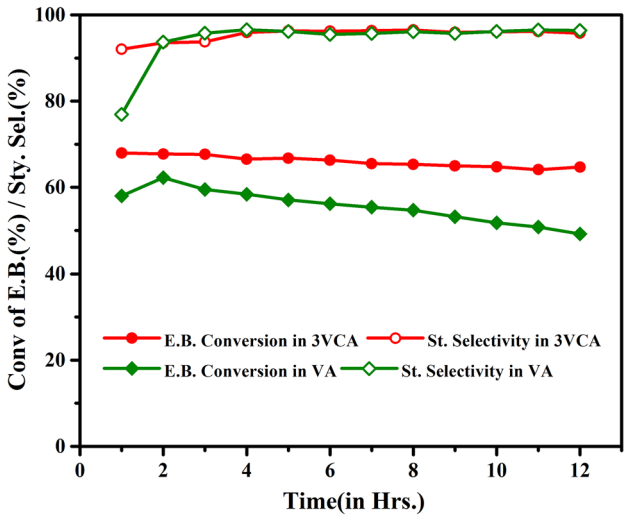

Fig. 7 Time on stream study over VA and 3VCA catalysts at 873 K

CeO_x addition increases the oxidizing power of the catalyst (CO_2 pulse chemisorption results). Further additions of CeO_x to VA (5VCA and 7VCA) showed no further increase in EB conversions. From these results, 3VCA was selected as optimum loading chosen for on stream studies. To understand the influence of CO_2 as a soft oxidant, the reaction was also carried out under N_2 flow on 3VCA under similar reaction conditions in the range of 723–923 K. The activity results with N_2 flow are far below than those with CO_2 flow. At 873 K, the EB conversion and ST selectivity are 57.3 and 95.6, respectively which are lower than those with CO_2 (EB conversion 69.1 % and ST selectivity 92.2 %). The lower EB conversion in N_2 feed is due to simple dehydrogenation reaction, while in the case of CO_2 feed gas better conversion and selectivity are due to the participation of both RWGSR and dehydrogenation reactions.

Since the catalysts were calcined at 773 K and tested in the temperature zone of 723–923 K, a set of catalysts were calcined at 973 K (above the reaction temperature) and these catalysts were characterized by XRD and TPR. The effect of reaction temperature on these catalysts was also performed. All the results have been shown in Electronic supplementary material (ES1for XRD figure, ES2 for TPR and ES3 for activity studies-temperature effect). Compared to the catalysts calcined at 773 K, the catalysts calcined at 973 K show slightly decreased activity; little bit more intense crystalline d-lines for ceria and slight shifting of T_{max} towards higher temperature were observed. These are due to the interaction between active phase/promoter with support. However, V_2O_5 remains in the highly dispersed form.

To understand the catalyst stability, time on stream experiment was performed with CO_2 feed gas for VA and

3VCA catalysts. On both VA and VCA catalysts, the major gaseous components observed are CO along with unconverted CO_2. H_2, CH_4, C_2H_6 are observed in minute quantities. Generally, a faster catalytic deactivation often was encountered in most of the catalytic systems in ODH reactions due to coke formation. Thus, time-on-stream study is very useful to understand the behavior of the catalysts. Figure 7 shows the effect of time-on-stream study in the presence of CO_2 feed gas at 873 K. From the figure, it is clear that during initial hours over VA, the conversion of EB increases from 58 to 62.2 %. The increase in conversion during initial hours is due to the formation of carbonaceous species over VA surface [44, 45]. Beyond second hour, the EB conversion decreases gradually and reaches 49.2 % at the end of 12th hour with an ST selectivity of 96 %. The presence of acidic sites prompts the formation of cracking products and thereby coke on the surface of the catalyst which results in decrease in the EB conversion. The continuous coke deposition on the surface of the catalyst is the major cause for the deactivation of the catalyst. The surface coke deposits hinder the adsorption of reactants on the active sites and in addition enhance the cracking by adsorption of the reactant on the coke present on the catalyst surface [44]. The activity of 3VCA catalyst shows almost stable EB conversion for 12 h (67–64 %) with 96 % ST selectivity. The activities of VA and 3VCA do not differ substantially during the initial hours. It is generally accepted that active sites for these systems are to be the surface vanadium cations operating according to a Mars-Van-Krevelen redox mechanism [33]. However, the catalyst stability is much improved by the addition of ceria to VO_X. It is suggested that easy redox cycle is an important factor to design more effective catalysts. Due to the addition of ceria to vanadia, the amount of reactive oxygen is increased and the reduction–reoxidation cycles of vanadium proceed more efficiently. The addition of ceria improved the catalytic activity in terms of conversion and improved the selectivity by minimizing the formation of coke deposition over the surface of catalyst. The stable activity of ceria-based catalysts is mainly due to facile oxygen transport from the bulk of CeO_2 [45–47]. Vanadium reduction from V^{5+} to V^{3+} also seems to be one of the main reasons of the deactivation of VA because the reoxidization of these strongly reduced active sites can become the rate-limiting step. This was confirmed by pulse and DSC techniques for the V_2O_5/Al_2O_3 catalyst for oxydehydrogenation of ethane [48].

Spent catalyst studies

The remarkable ability of CeO_2 in V_2O_5/Al_2O_3 catalysts to obtain a high and stable activity is clearly apparent from the present study. To understand the deactivation phenomenon of these catalysts, the spent catalysts were subjected to XRD and TPR analysis. XRD patterns for the spent catalysts (collected after time on stream study over VA and 3VCA) are shown in Fig. 8. Peaks correspond to ceria and alumina retained and there is no such noticeable change in the peak positions or their intensities after TOS indicating that the structure is retained even after 12 h reaction. In fresh catalysts, no peaks corresponding to vanadia were observed both in VA and 3VCA. The diffraction peaks corresponding to vanadia are absent in the XRD patterns of spent catalysts which indicates that vanadia retains its amorphous nature in both VA and 3VCA catalysts after 12 h reaction.

TPR patterns of the fresh VA and 3VCA catalysts (Fig. 9) show two T_{max} values at 803,943 K for VA and 843, 983 K for 3VCA catalysts, respectively. While the spent catalysts show the same two-stage reducibility with

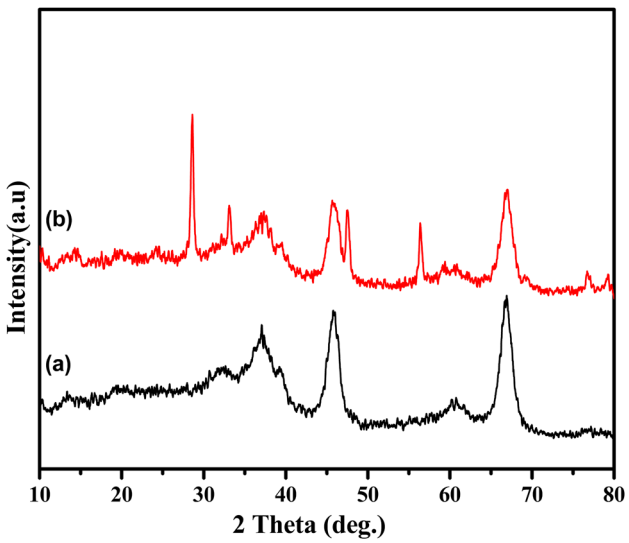

Fig. 8 Powder XRD patterns for *a* VA, *b* VA spent, *c* 3VCA, and *d* 3VCA spent catalysts

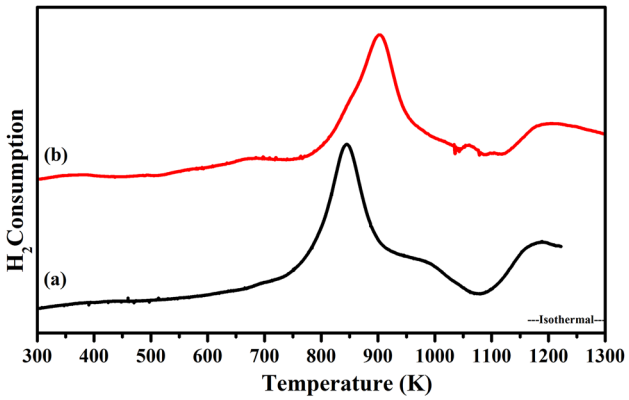

Fig. 9 TPR patterns for *a* VA and *b* 3VCA spent catalysts

Table 2 Comparison of ethylbenzene dehydrogenation activity of various catalysts with the present catalyst

Catalyst	Feed flow	Reaction conditions	Ethylbenzene conversion (%)	Styrene selectivity (%)	Refs.
VSbO*x*/Al2O3	CO_2	868 K, 1 atm	79.9	95.1	[37]
V_2O_5/MgO	CO_2	823 K, 1 atm	73.8	90.1	[7]
CeO_2-V_2O_5/TiO_2-ZrO_2	CO_2	823 K, 1 atm	56	98	[47]
V_2O_5/CeO_2/Al_2O_3	CO_2	723 K, 1 atm	19	94	[39]
CeO_2 cubes	CO_2	833 K, 1 atm	58	80	[21]
V_2O_5/activated carbon	CO_2	823 K, 1 atm	52	97.3	[8]
V_2O_5/CeO_2-Al_2O_3	CO_2	873 K, 1 atm	68.4	92.2	Present

higher T_{max} values. The increase in T_{max} values is ascribed to the formation of coke deposition on the surface of the catalyst which will hinder the reducibility of a catalyst by forming a carbon layer on the surface of the support. Along with these two peaks, one more negative peak was observed at around 1073 K in both the catalysts. This negative peak might be due to the reduction of H_2-rich CH_X species formed during the reaction [36, 49].

The CHNS results indicate that the rate of formation of carbon in the spent VA catalyst is 1.48 mmol-Carbon/h/gm catalyst which is much higher than that on 3 VCA catalyst (0.92 mmol-Carbon/h/gm catalyst). Coking of catalysts generally occurs due to cracking products. The addition of ceria to VA results in low coke formation, which suggests that the ceria is preventing the coke formation by decreasing the formation of side products.

Activity comparison with reported catalysts

Table 2 presents the comparison of activity of different catalysts cited in the literature with the present catalyst system for EB dehydrogenation with CO_2. It was reported that SbO_X species increases the redox capability of V_2O_5 on Al_2O_3 which in turn increases the EB conversion with high ST selectivity [12]. It appears that the role of CeO_X in the present case is similar to that of SbO_X. It was reported that V_2O_5 supported on MgO catalyst exhibited high initial EB conversion with high ST selectivity, but suffers reduction in the ST yield with in 6 h [7]. The advantage of CeO_X on V_2O_5/TiO_2-ZrO_2 catalyst in maintaining steady EB conversion with high ST selectivity for a period of 10 h time on stream study was reported [46]. Another study highlighted the advantage of CeO_X to V_2O_5/Al_2O_3 catalyst in promoting the EB conversion in CO_2 at low temperatures [38]. Another study indicated that among different phases of CeO_X, CeO_2 cubes are active for EB dehydrogenation [21]. Comparison of [21] with [8] indicates that vanadia's role is in maintaining higher selectivity to ST than with CeO_X. Thus, the EB dehydrogenation activity of the present catalyst system, 3VCA, is either on par or more active compared to the reported catalysts.

Conclusions

XRD results indicate that VO_X species are present either in amorphous phase or highly dispersed on the surface of the support. TPR results suggest that the increased T_{max} values in VCA catalysts compared to VA catalyst are due to the interactions between ceria and VO_x species. CO_2 TPD results suggest that the addition of ceria to VO_X-Al_2O_3 increased their basicity. CO_2 pulse chemisorption studies indicate that the addition of ceria increased the redox properties of VO_X component. The addition of 3 % ceria to VO_x/Al_2O_3 is helpful in not only improving the catalytic activity but also yielding stable results up to 12 h during time on stream studies. The stable and high catalytic activity of ceria-incorporated VO_x/Al_2O_3 catalysts is mainly due to the facile oxygen transport from bulk of CeO_2.

Acknowledgments GVRB and ESS acknowledge the Department of Science and Technology (DST), Government of India, New Delhi for the award of fellowship and all authors are grateful to DST for sanctioning a project (Project No. DST/IS-STAC/CO_2-SR-136/12(G)).

References

1. Meima GR, Menon PG (2001) Catalyst deactivation phenomena in styrene production. Appl Catal A Gen 212:239–245
2. Cavani F, Trifiro F (1995) Alternative processes for the production of styrene. Appl Catal A Gen 133:219–239
3. Jiang N, Han DS, Park SE (2009) direct synthesis of mesoporous silicalite-1 supported TiO_2-ZrO_2 for the dehydrogenation of ethylbenzene to styrene with CO_2. Catal Today 141:344–348
4. Chang JS, Park SE, Park MS (1997) Beneficial effect of carbon dioxide in dehydrogenation of ethylbenzene to styrene over zeolite-supported iron oxide catalyst. Chem Lett 26:1123–1124
5. Sugino M, Shimada H, Turuda T, Miura H, Igenaga N, Suzuki T (1995) Oxidative dehydrogenation of ethylbenzene with carbon dioxide. Appl Catal A Gen 121:125–137

6. Sakurai Y, Suzaki T, Nakagawa K, Ikenaga NO, Aota H, Suzuki T (2000) Oxidation capability of carbon dioxide in the dehydrogenation of ethylbenzene over vanadium oxide-loaded MgO catalyst. Chem Lett 29:526–527
7. Sakurai Y, Suzaki T, Nakagawa K, Ikenaga NO, Aota H, Suzuki T (2002) Dehydrogenation of ethylbenzene over vanadium oxide-loaded MgO catalyst: promoting effect of carbon dioxide. J Catal 209:16–24
8. Chen S, Qin Z, Sun A, Wang J (2006) Theoretical and experimental study on reaction coupling: dehydrogenation of ethylbenzene in the presence of carbon dioxide. J Nat Gas Chem 15:11–20
9. Christian N, Valeriya Z, Ignacio VMC, Erik HJH, Freek K, Michiel M (2014) Application of staged O_2 feeding in the oxidative dehydrogenation of ethylbenzene to styrene over Al_2O_3 and P_2O_5/SiO_2 catalysts. Appl Catal A Gen 476:204–214
10. Christian N, Valeriya Z, Ignacio MC, Hero JH, Freek K, Michiel M (2013) Oxidative dehydrogenation of ethylbenzene to styrene over alumina: effect of calcination. Catal Sci Technol 3:519–526
11. Zarubina V, Nederlof C, Van der Linden B, Kapteijn F, Heeres HJ, Makkee M, Melian-Cabrera I (2014) Making coke a more efficient catalyst in the oxidative dehydrogenation of ethylbenzene using wide-pore transitional aluminas. J Mol Cat A Chem 381:179–187
12. Park ME, Vislovskiy VP, Chang JS, Shul YG, Yoo JS, Park SE (2003) Catalytic dehydrogenation of ethylbenzene with carbon dioxide: promotional effect of antimony in supported vanadium–antimony oxide catalyst. Catal Today 87:205–212
13. Sato S, Ohhara M, Sodesawa T, Nozaki F (1988) Combination of ethylbenzene dehydrogenation and carbon dioxide shift-reaction over a sodium oxide/alumina catalyst. Appl Catal A Gen 37:207–215
14. Matsui J, Sodesawa T, Nozaki F (1990) Influence of carbon dioxide addition upon decay of activity of a potassium-promoted iron oxide catalyst for dehydrogenation of ethylbenzene. Appl Catal A Gen 67:179–188
15. Mimura N, Saito M (1999) Dehydrogenation of ethylbenzene to styrene over Fe_2O_3/Al_2O_3 catalysts in the presence of carbon dioxide. Catal Lett 58:59–62
16. de Morais Batista A H, de Sousa FF, Honorato SB, Ayala AP, Filho JM, de Sousa FW, Pinheiro AN, de Araujo JCS, Nascimento RF, Valentini A, Oliveira AC (2010) Ethylbenzene to chemicals: catalytic conversion of ethylbenzene into styrene over metal-containing MCM-41. J Mol Catal A: Chem 315:86–98
17. Rao KN, Reddy BM, Park SE (2010) Novel CeO_2 promoted TiO_2–ZrO_2 nano-oxide catalysts for oxidative dehydrogenation of p-diethylbenzene utilizing CO_2 as soft oxidant. Appl Catal B Environ 100:472–480
18. Lisovskii AE, Aharoni C (1994) Carbonaceous deposits as catalysts for oxydehydrogenation of Alkylbenzenes. Catal Rev Sci Eng 36:25–74
19. Burri A, Jiang N, Yahyaoui K, Park SE (2015) Ethylbenzene to styrene over alkali doped TiO_2-ZrO_2 with CO_2 as soft oxidant. Appl Catal A Gen 495:192–199
20. Sanz SG, McMillan L, McGregor J, Zeitler JA, Al Yassir N, Al Khattafb S, Gladdena LF (2016) The enhancement of the catalytic performance of CrO_x/Al_2O_3 catalysts for ethylbenzene dehydrogenation through tailored coke deposition. Catal Sci Technol 6:1120–1133
21. Kovacevic M, Agarwal S, Mojet BL, van Ommen Jan G, Lefferts L (2015) The effects of morphology of cerium oxide catalysts for dehydrogenation of ethylbenzene to styrene. Appl Catal A Gen 505:354–364
22. Shiju NR, Anilkumar M, Mirajkar SP, Gopinath CS, Rao BS, Satyanarayana CV (2005) Oxidative dehydrogenation of ethylbenzene over vanadia-alumina catalysts in the presence of nitrous oxide: structure-activity relationship. J Catal 230:484–492
23. Chen S, Qin Z, Xu X, Wang J (2006) Structure and properties of the alumina-supported vanadia catalysts for ethylbenzene dehydrogenation in the presence of carbon dioxide. Appl Catal A Gen 302:185–192
24. Itika K, Jayesh TB, Rangappa SK, Nagaraja BM (2015) Activity studies of vanadium, iron, carbon and mixed oxides based catalysts for the oxidative dehydrogenation of ethylbenzene to styrene: a review. Catal Sci Technol 5:5062–5076
25. Reddy BN, Reddy BM, Subrahmanyam M (1991) Dispersion and 3-picoline ammoxidation investigation of V_2O_5/α-Al_2O_3 catalysts. J Chem Soc, Faraday Trans 87:1649–1655
26. Imamura S, Fakuda I, Ishida S (1988) Wet oxidation catalyzed by ruthenium supported on cerium (IV) oxides. Ind Eng Chem Res 27:718–721
27. Mishra VS, Mahajani VV, Joshi JB (1995) Wet air oxidation. Ind Eng Chem Res 34:2–48
28. Trovarelli A, Dolcetti G, de Leitenburg C, Kaspar J, Finetti P, Santoni A (1992) Rh-CeO_2 interaction induced by high-temperature reduction. Characterization and catalytic behavior in transient and continuous conditions. J Chem Soc, Faraday Trans 88:1311–1319
29. Reddy BM, Lakshmanan P, Bharali P, Saikia P, Thrimurthulu G, Muhler MGrunert W (2007) Influence of alumina, silica, and titania supports on the structure and CO oxidation activity of $Ce_xZr_{1-x}O_2$ nanocomposite oxides. J Phys Chem C111:10478–10483
30. Monteiro RS, Dieguez LC, Schmal M (2001) The role of Pd precursors in the oxidation of carbon monoxide over Pd/Al_2O_3 and $Pd/CeO_2/Al_2O_3$ catalysts. Catal Today 65:77–89
31. Zhang H, Zhu A, Wang X, Wang Y, Shi C (2007) Catalytic performance of Ag–Co/CeO_2 catalyst in NO-CO and NO-CO-O_2 system. Catal Commun 8:612–618
32. Andreeva D, Ivanov I, Ilieva L, Abrashov MV (2006) Gold catalysts supported on ceria and ceria-alumina for water-gas shift reaction. Appl Catal A Gen 302:127–132
33. Trovarelli A, Leitenburg C, Dolcetti G (1997) Design better cerium based oxidation catalysts. Chem tech 27:32–37
34. Ramudu P, Anand N, Venkata RBG, Murali DG, Sai Prasad PS, David Raju B, Seetha Rama Rao K (2014) Molybdenum oxide supported on COK-12: a novel catalyst for oxidative dehydrogenation of ethylbenzene to styrene using CO_2. Indian J Chem 53A:493–498
35. Ramudu P, Anand N, Mohan V, Murali DG, Sai Prasad PS, David Raju B, Seetha Rama Rao K (2015) Studies on ethylbenzene dehydrogenation with CO_2 as soft oxidant over Co_3O_4/COK^{-12} catalysts. J ChemSci 127:701–709
36. Madhavi J, Suresh M, Ramesh Babu GV, Sai Prasad PS, David Raju B, Rama Rao KS (2014) N_2 as a co-soft oxidant along with CO_2 in ethylbenzene dehydrogenation to styrene over γ-Al_2O_3 supported Co-Mo nitride catalysts. J CO2 Util 8:21–26
37. Beitha MA, Rabie AM, Elfadl AM, Yehia FZ (2016) microwave assisted synthesis of a VO_x modified disordered mesoporous silica for ethylbenzene dehydrogenation in presence of CO_2. Microporous Mesoporous Mater 222:44–54
38. Reddy BM, Rao KN, Reddy GK, Khan A, Park SE (2007) Structural characterization and oxidehydrogenation activity of CeO_2/Al_2O_3 and $V_2O_5/CeO_2/Al_2O_3$ catalysts. J Phy Chem C111:18751–18758
39. Roozeboom F, Mittelmeijer-Hazeleger MC, Moulijn JA, Medema J, de Beer VHJ, Gellings PJ (1980) Vanadium oxide monolayer catalysts. 3. A Raman spectroscopic and temperature-programmed reduction study of monolayer and crystal-type vanadia on various supports. J Phys Chem 84:2783–2791

40. Erdohelyi A, Solymosi F (1991) Oxidation of ethane over silica-supported alkali metal vanadate catalysts. J Catal 129:497–510
41. Lemonidou AA, Nalbandian L, Vasalos IA (2000) Oxidative dehydrogenation of propane over vanadium oxide based catalysts: effect of support and alkali promoter. Catal Today 61:333–341
42. Liu YM, Cao Y, Yi N, Feng WL, Dai WL, Yan SR, He HY, Fan KN (2004) Vanadium oxide supported on mesoporous SBA-15 as highly selective catalysts in the oxidative dehydrogenation of propane. J Catal 224:417–428
43. Reddy EP, Varma RS (2004) Preparation, characterization, and activity of Al2O3-supported V2O5 catalysts. J Catal 221:93–101
44. Fiedorow R, Przystajko W, Sopa M, Dalla LanaI G (1981) The nature and catalytic influence of coke formed on alumina: oxidative dehydrogenation of ethylbenzene. J Catal 68:33–41
45. Murugan B, Ramaswamy AV (2007) Defect-site promoted surface reorganization in nanocrystalline ceria for the low-temperature activation of ethylbenzene. J Am Chem Soc 129:3062–3063
46. Reddy BM, Lee SC, Han DS, Park SE (2009) Utilization of carbon dioxide as soft oxidant for oxidehydrogenation of ethylbenzene to styrene over V_2O_5–CeO_2/TiO_2–ZrO_2 catalyst. Appl Catal B Environ 87:230–238
47. Rao KN, Reddy BM, Abhishek B, Seo YH, Jiang N, Park SE (2009) Effect of ceria on the structure and catalytic activity of V_2O_5/TiO_2–ZrO_2 for oxidehydrogenation of ethylbenzene to styrene utilizing CO_2 as soft oxidant. Appl Catal B Environ 91:649–656
48. Le Bars J, Auroux A, Forissier M, Vedrine JC (1996) Active sites of V_2O_5/γ-Al_2O_3 catalysts in the oxidative dehydrogenation of ethane. J Catal 162:250–259
49. Chandra Shekar S, Krishna Murthy J, Kanta Rao P, Rama Rao KS (2003) Selective hydrogenolysis of dichlorodifluoromethane on carbon covered alumina supported palladium catalyst. J Mol Catal A: Chem 191:45–59